XIX Seminarium

ZASTOSOWANIE KOMPUTERÓW W NAUCE I TECHNICE' 2009
Oddział Gdański PTETiS
Referat nr 29

NONLINEAR MODELING OF TRACTION TRANSFORMER WITH COILED IRON CORE FOR DYNAMIC SIMULATION

Andrzej WILK

Politechnika Gdańska, ul. G. Narutowicza 11/12, 80-952 Gdańsk,
tel: 058 347 1087, fax: 058 341 0880, e-mail: awilk@ely.pg.gda.pl

Abstract: The paper presents development of an equivalent circuit model of a traction transformer with coiled iron core intended for studies of transformer behavior in a traction drive system. The model accounts for the nonlinear B-H characteristic and anisotropic properties of the coiled core. Derivation of the model is based on the Lagrange's energy method. Each winding is modeled by a lumped conservative element described by its corresponding nonlinear state function and a lumped linear dissipative element characterized by its resistance. Discrete values of state functions of magnetic conservative elements were obtained by finite element computations. Custom build Reduced Scale Traction Transformer (RSTT) was used for experiments and verification of its circuit mathematical model. Results of measurements and simulations were compared to verify the model. The comparisons showed good agreement between simulation and experimental results.

Key-words: traction transformer, nonlinear model, coiled core.

1. INTRODUCTION

Main traction transformers are single-phase multi-winding devices. They usually have from 8 to 16 windings. The number of windings depends mainly on the motor type used and the power of train. A traction transformer core is made up of electrical steel laminations stacked together. Such a core structure has mitered regions formed by overlapping steel sheets which have worse magnetic properties than regions in yokes and limbs [1]. A coiled (wound) iron core is an alternative approach used in power transformers [2].

Modeling of traction transformers is very important for simulations and analysis of transient states in power trains. The exact circuit parameters are needed for proper control strategy of drive systems. The key point of transformer modeling is the representation of nonlinear magnetization and anisotropy of the iron core in calculation based on Finite Element Method [3]. Experimental results of single phase wound transformers [4,5] show complexity of longitudinal and normal flux distribution under alternating magnetization. There have been few attempts to model each individual steel sheet and varnish between sheets of wound core [6] but only in 2D field analysis and for a small number of sheets. For large scale 3D FEM modeling an iron-laminated core as homogenous material is considered instead [7].

In this paper an eight winding transformer with tape wound iron core is studied. The iron core is treated as nonlinear and anisotropic homogenous material. A schematic representation of the primary and secondary windings in the considered transformer is shown in figure 1. The geometrical positions of the coils in the transformer are depicted in figure 2. The primary windings are made of three parallel sections. The coils denoted P2 and P4 make two sections of the primary traction winding. The coils denoted P1 and P3, connected in series inside the transformer, form a single section referred to as the primary auxiliary winding. The coils labeled T1 and T2, not connected inside the transformer, form two sections of the traction secondary winding. The coils S1 and S2, connected in series inside the transformer, are the auxiliary secondary winding.

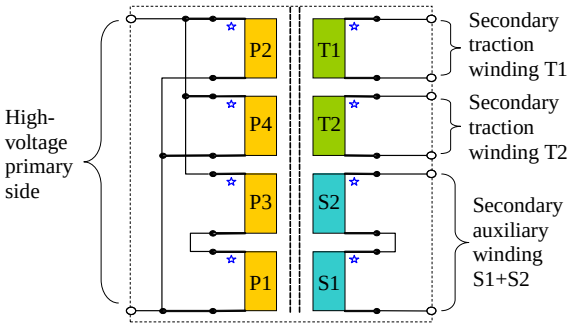

Fig.1. Schematic representation of sections, coils, and their connections in the considered traction transformer

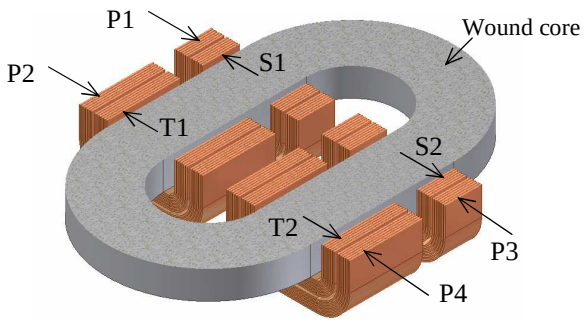

Fig.2. Isometric view of cross section of the considered transformer and arrangement of its windings: primary P1,P2,P3,P4 and secondary S1,S2,T1,T2

Recenzent: Prof. dr hab. inż. Paweł Zimny – Wydział Elektrotechniki i Automatyki Politechnika Gdańska

2. CIRCUIT MODEL OF THE TRANSFORMER

An equivalent circuit of the considered transformer supplied from an ideal voltage source and non-reactive loading is shown in figure 3.

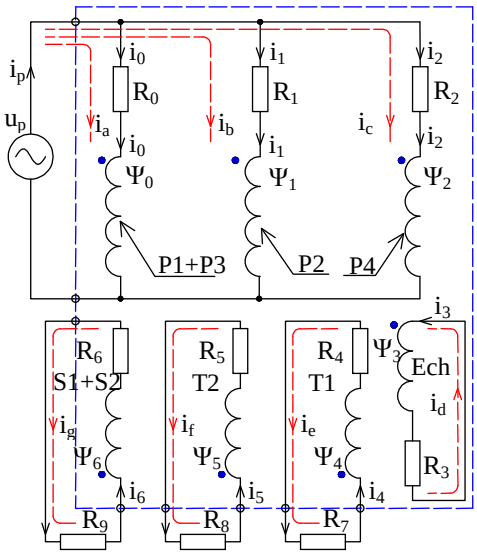

Fig.3. Circuit representation of the considered transformer supplied from an ideal voltage source and non-reactive loading

The traction primary windings (P1+P3,P2,P4) are energized from an AC source with the voltage $u_p(t)$. A single equivalent circuit Ech for modeling hysteresis and eddy currents losses is assumed. Windings T1, T2, and S1+S2 are loaded by the following resistors R_7, R_8, R_9 respectively. The rest of particular symbols are as follows: Ψ_0 - flux linkage of P1+P3 windings; Ψ_1 - flux linkage of P2 winding; Ψ_2 - flux linkage of P4 winding; Ψ_3 - flux linkage of eddy currents and hysteresis equivalent loop; Ψ_4 - flux linkage of T1 winding; Ψ_5 - flux linkage of T2 winding; Ψ_6 - flux linkage of S1+S2 windings; R_0 – resistance of P1+P3 windings; R_1 – resistance of P2 winding; R_2 – resistance of P4 winding; R_3 – resistance of eddy currents loop; R_4, R_5 – resistances of T1 and T2 windings respectively; R_6 – resistance of S1+S2 windings.

Mathematical description of the equivalent circuit shown in figure 3 that takes into account all magnetic couplings between the transformer windings has the following form:

$$\mathbf{C}^{\mathrm{T}}\begin{bmatrix} \frac{\partial}{\partial i_0}\Psi_0(i_0,\ldots,i_6) & \cdots & \frac{\partial}{\partial i_6}\Psi_0(i_0,\ldots,i_6) & 0 & \cdots & 0 \\ \frac{\partial}{\partial i_0}\Psi_1(i_0,\ldots,i_6) & \cdots & \frac{\partial}{\partial i_6}\Psi_1(i_0,\ldots,i_6) & 0 & \cdots & 0 \\ \vdots & \cdots & \vdots & \vdots & \cdots & 0 \\ \frac{\partial}{\partial i_0}\Psi_6(i_0,\ldots,i_6) & \cdots & \frac{\partial}{\partial i_6}\Psi_6(i_0,\ldots,i_6) & 0 & \cdots & 0 \\ 0 & \cdots & 0 & 0 & \cdots & 0 \\ \vdots & \cdots & \vdots & \vdots & \ddots & 0 \\ 0 & \cdots & 0 & 0 & \cdots & 0 \end{bmatrix}\mathbf{C}\frac{d}{dt}\begin{bmatrix} i_a \\ i_b \\ i_c \\ i_d \\ i_e \\ i_f \\ i_g \end{bmatrix}+$$

$$+\mathbf{C}^{\mathrm{T}}\begin{bmatrix} R_0 & 0 & \cdots & 0 & 0 \\ 0 & R_1 & \cdots & 0 & 0 \\ \vdots & \vdots & \ddots & \vdots & \vdots \\ 0 & 0 & \cdots & R_8 & 0 \\ 0 & 0 & \cdots & 0 & R_9 \end{bmatrix}\mathbf{C}\begin{bmatrix} i_a \\ i_b \\ i_c \\ \vdots \\ i_g \end{bmatrix}=\begin{bmatrix} U_p(t) \\ U_p(t) \\ U_p(t) \\ 0 \\ \vdots \end{bmatrix} \qquad (1)$$

where **C** is the matrix of constraints linking the non-generalized coordinates $\begin{bmatrix} i_0 & i_1 & \cdots & i_9 \end{bmatrix}^T$ and the generalized coordinates $\begin{bmatrix} i_a & i_b & \cdots & i_g \end{bmatrix}^T$. The relation between these coordinates using the matrix **C** is given as

$$\begin{bmatrix} i_0 & i_1 & \cdots & i_9 \end{bmatrix}^T = \mathbf{C}\begin{bmatrix} i_a & i_b & \cdots & i_g \end{bmatrix}^T \qquad (2)$$

The way of development of the model including description of the matrix of constraints is presented in [8]. Each winding is modeled as the lumped conservative element described by its corresponding nonlinear state function $\Psi_k(i_0,\ldots,i_6)$ and dissipative element characterized by its resistance R_k, where k = 0,1,2, …, 6 identifies the lumped elements as shown in figure 3. The equivalent resistance R_3 is nonlinear in other to obtain good agreement between recorded and simulated shapes of exciting currents. All other resistances are assumed to be linear.

3. CALCULATION OF CIRCUIT PARAMETERS

Field simulations were performed in commercial FEM software Opera3D using steady-state alternating currents (Elektra) solver with the following assumptions: B-H is a non-hysteretic curve; the relative magnetic permeability in the direction normal to the lamination is approximately equal to one. The grain oriented silicon steel ET114 type (with the thickness of 0.27 mm) was used in simulations.

3.1. 3D FE formulation

The calculation problem is defined within three domains (Ω_1, Ω_2, Ω_3) as shown in figure 4. The Ω_1 domain is the volume of all windings, Ω_2 is the volume of the wound core, and Ω_3 corresponds to air surrounding the windings and the core.

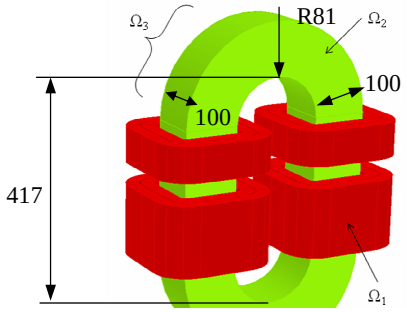

Fig.4. 3D model of the transformer showing its main dimensions (in millimeters) and three computational domains

The Maxwell's equations for defined domains have the form

$$\nabla\times\mathbf{H}=\begin{cases}\mathbf{j} & in\ \Omega_1\\ \ddot{\boldsymbol{\sigma}}\mathbf{E} & in\ \Omega_2;\\ 0 & in\ \Omega_3\end{cases}\qquad \nabla\times\mathbf{E}=-\frac{\partial\mathbf{B}}{\partial t};\quad \nabla\bullet\mathbf{B}=0;\quad \mathbf{B}=\nabla\times\mathbf{A} \qquad (3)$$

where $\ddot{\boldsymbol{\sigma}}$ is the electrical conductivity tensor

$$\ddot{\boldsymbol{\sigma}}=\begin{bmatrix}\sigma_{xx}(x,y,z) & 0 & 0\\ 0 & \sigma_{yy}(x,y,z) & 0\\ 0 & 0 & \sigma_{zz}(x,y,z)\end{bmatrix} \qquad (4)$$

The permeability tensor $\ddot{\boldsymbol{\mu}}$ which for nonlinear properties describes the relation between **dB** and **dH** in constitutive equation can be expressed as

$$\ddot{\boldsymbol{\mu}} = \begin{cases} \mu_0 & in\ \Omega_1 \\ \ddot{\boldsymbol{\mu}}_{core} & in\ \Omega_2; \\ \mu_0 & in\ \Omega_3 \end{cases} \quad \ddot{\boldsymbol{\mu}}_{core} = \begin{bmatrix} \mu_{xx}(x,y,z) & 0 & 0 \\ 0 & \mu_{yy}(x,y,z) & 0 \\ 0 & 0 & \mu_{zz}(x,y,z) \end{bmatrix} \tag{5}$$

Simulation of anisotropy in Opera3D software is based on the use of materials' functional volume properties. Volume labels were specified for limbs and yokes. Next, for each volume label, the Euler angles were defined as variables of x,y,z coordinates to establish required permeability and conductivity in the axial, tangential, and normal direction of the lamination as shown in figure 4.

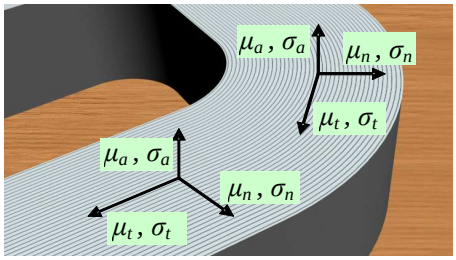

Fig.4. Specification of permeability μ and conductivity σ in the axial (a), tangential (t), and normal (n) direction of the wound core

Using local axial-tangential-normal (a,t,n) coordinates the permeability and conductivity tensors can be written as

$$\ddot{\boldsymbol{\mu}}_{core} = \begin{bmatrix} \mu_a = \dfrac{dB}{dH} & 0 & 0 \\ 0 & \mu_t = \dfrac{dB}{dH} & 0 \\ 0 & 0 & \mu_n \approx \mu_0 \end{bmatrix}; \quad \ddot{\boldsymbol{\sigma}} = \begin{bmatrix} \sigma_a & 0 & 0 \\ 0 & \sigma_t & 0 \\ 0 & 0 & \sigma_n \end{bmatrix} \tag{6}$$

The following values are assumed: $\sigma_a = \sigma_t$=5E6 S/m, σ_n=100 S/m. The B-H non-hysteretic curve is shown in figure 5.

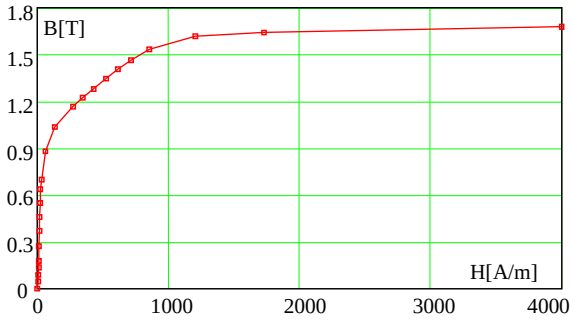

Fig.5. B-H non-hysteretic curve of the steel ET114 type measured by the author on a toroidal sample

3.2. State functions and inductances of the transformer

The field distribution results were presented in [9]. Discrete values of state functions have been obtained by integration of flux density distribution. Figure 6 shows the family of linkage fluxes of the winding P2 as a function of $i_{P2},i_{T1},i_{P1},i_{S1},i_{P3},i_{P4},i_{S2},i_{T2}$ ampere-turns of particular windings. This and similar results for other windings enable to obtain the mutual linkage flux as a function of all exciting currents and leakage fluxes of particular windings. Then continuous representations of these functions were obtained using cubic spline piecewise interpolation. Derivatives of linkage fluxes with respect to particular winding currents give self and mutual inductances as shown in figure 7 for the winding P2.

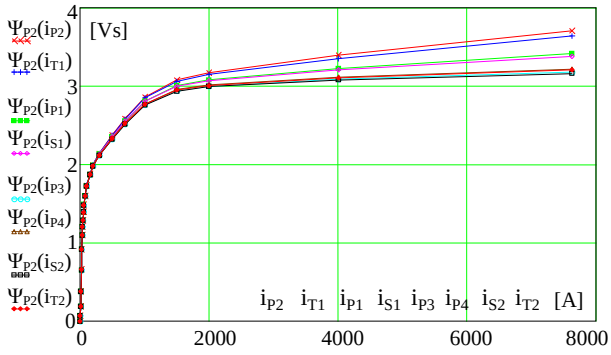

Fig.6. Family of fluxes of the winding P2 as a function of $i_{P2},i_{T1},i_{P1},i_{S1}$, $i_{P3},i_{P4},i_{S2},i_{T2}$ ampere-turns of particular winding currents

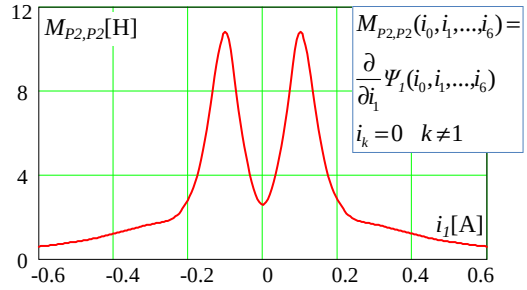

Fig.7. Self inductance of the winding P2 as a function of the current i_1 ; values of other currents were equal to zero

4. COMPARISON OF SIMULATION AND MEASUREMENT RESULTS

For experiments a custom build Reduced Scale Traction Transformer (RSTT) was used (Fig.8). Its model is considered in the paper. Comparison between simulated and measured exciting currents for no-load operation of the transformer is presented in figure 9.

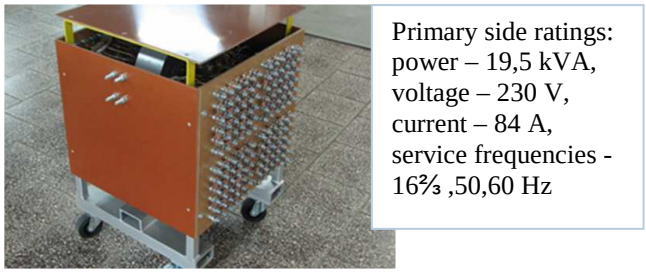

Fig.8. View of the RSTT and its primary side ratings

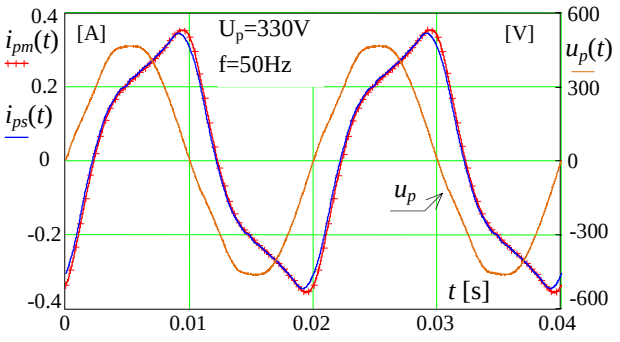

Fig.9. Comparison between simulated i_{ps} and measured i_{pm} exciting currents for no-load operation of the RSTT

Nonlinear magnetic property and magnetic saturation influence the inrush current. Figure 10 shows the result of inrush current simulation of the RSTT supplied with the nominal sinusoidal voltage at frequency equal to 16⅔ Hz.

The influence of hysteresis and eddy currents effects on mutual linkage flux can be measured as shown in the figure 11 in case of the winding P2. The characteristics of linkage flux Ψ_{P2} as a function of the exciting current i_p create loops. For comparison the non-hysteretic state function of the winding P2 is added. The areas of these loops represent the energy dissipated on equivalent R_3 resistance and can be used for its verification or calculation.

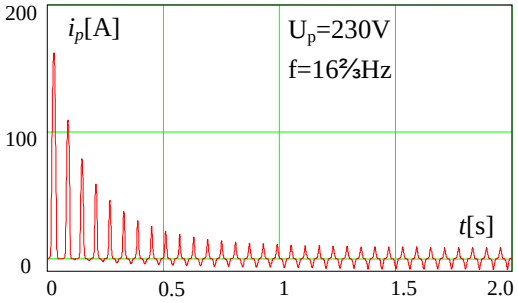

Fig.10. Result of inrush current simulation of the RSTT supplied with nominal sinusoidal voltage at frequency equal to 16⅔ Hz

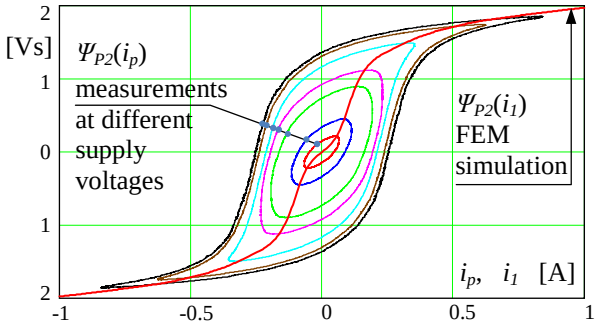

Fig.11. Linkage fluxes of the winding P2 as functions of exciting currents i_p at different supply voltages

5. CONCLUSION

The state function of each lumped magnetic element of the considered transformer can be represented by the nonlinear mutual linkage flux and the sum of particular leakage fluxes. Cubic spline piecewise interpolation is a very good approach to approximate highly nonlinear discreet state functions. Verification examples show correctness and accuracy of the developed circuit model of the RSTT for steady state and dynamic simulations.

5. REFERENCES

1. Jones M.A., Moses A.J.: Comparison of the localized power loss and flux distribution in the butt and lap and mitred overlap corner configurations, IEEE Transactions on Magnetics, Vol. 10, No. 2, June 1974, pp. 321-326.
2. Kefalas T.D., Georgilakis P.S., Kladas A.G. Souflaris A.T., Paparigas D.G.: Multiple grade laminations wound core: A novel technique for transformer iron loss minimization using simulated annealing with restarts and anisotropy model, IEEE Transactions on Magnetics, Vol. 44, No. 6, June 2008, pp. 1082-1085.
3. Mohammed O.A., Liu Z., Liu S., Abed N.Y.: Finite-element-based nonlinear physical model of iron-core transformers for dynamic simulations, IEEE Transactions on Magnetics, Vol. 42, N0. 4, April 2006, pp. 1027-1030.
4. Enokizono M., Rokada T., Nakamura K.: Flux distribution in a wound core of of a single-phase transformer, Journal of Magnetism and Magnetic Materials, Vol. 160, July 1996, pp. 61-62.
5. Loizos G., Kefalas A.K., Souflaris T., Paparigas D.: Flux distribution in single phase, Si-Fe, wound transformer cores, Journal of Magnetism and Magnetic Materials, Vol. 320, 20 Oct. 2008, pp. e874-e877.
6. Zurek S., Al-Naemi F., Moses A.J.: Finie-element modeling and measurements of flux and eddy current distribution in toroidal cores wound from electrical steel, IEEE Transactons on Magnetics, Vol. 44, No. 6, June 2008, pp. 902-905.
7. Kefalas T.D., Kladas A.G.: Robust numerical analysis of wound core distribution transformers, 18th International Conference on Electrical Machines ICEM2008, 6-7 Sept. 2008, Vilamoura (Portugal), pp. 1-6, Paper ID 1425.
8. Sobczyk T.: Metodyczne aspekty modelowania matematycznego maszyn indukcyjnych, Warszawa WNT 2004, s. 38-66, ISBN 83-204-2886-6.
9. Wilk A., Nieznanski J., Moson I., Dobrowolski P., Kostro G.: Nonlinear equivalent circuit model of a traction transformer for winding internal fault diagnostic purposes, 18th International Conference on Electrical Machines ICEM2008, 6-7 Sept. 2008, Vilamoura (Portugal), pp. 1-6, Paper ID 1207.

NIELINIOWE MODELOWANIE TRANSFORMATORA TRAKCYJNEGO Z ŻELAZNYM RDZENIEM ZWIJANYM DO DYNAMICZNYCH SYMULACJI

Słowa kluczowe: transformator trakcyjny, model nieliniowy, rdzeń zwijany

W artykule przedstawiono model obwodowy transformatora trakcyjnego z rdzeniem zwijanym przeznaczonego do badań trakcyjnego układu napędowego. Model zakłada nieliniowość charakterystyki B-H oraz anizotropowe właściwości rdzenia zwijanego. Model został wyprowadzony w oparciu o metodę energetyczną Lagrange'a. Model obwodowy jest reprezentowany przez układ nieliniowych elementów zachowawczych i dyssypatywnych. Dyskretne wartości funkcji stanu elementów magnetycznych otrzymano z symulacji polowej. Zbudowany od podstaw transformator trakcyjny o zredukowanej skali został użyty jako obiekt modelowania i weryfikacji modelu matematycznego. Wyniki pomiarów i symulacji obwodowej porównano w celu weryfikacji modelu. Porównanie wykazało dobrą zgodność wyników symulacji i eksperymentów.